

**Stable, polymer-directed and SPION-nucleated magnetic
amphiphilic block copolymer nanoprecipitates with readily
reversible assembly in magnetic fields.**

Marco Giardiello, Fiona L. Hatton, Rebecca A. Slater, Pierre Chambon, Jocelyn North, Anita Peacock,
Tom O. McDonald, Andrew Owen, and Steve. P. Rannard.*

Department of Chemistry, University of Liverpool, Crown Street, Liverpool, L69 7ZD, UK

E-mail: srannard@liverpool.ac.uk

Supplementary Information

Materials

2-Hydroxypropyl methacrylate (HPMA) 97 %, ethylene glycol dimethacrylate (EGDMA) 98 %, ethyl-2-bromoisobutyrate (EBiB) 98%, 2-bromoisobutryl bromide 98%, monomethoxy-polyethylene glycol (nominal $M_n = 750, 2000, 5000 \text{ g mol}^{-1}$), Cu(I)Cl >99 %, 2,2',-bipyridyl >99 %, aluminium oxide (activated, basic), Iron(III) chloride hexahydrate ($\text{FeCl}_3 \cdot 6\text{H}_2\text{O}$), oleic acid (90%), 1-octadecene (90%), Dowex Marathon exchange resin, 4-(dimethylamino) pyridine >98 %, triethylamine (TEA) >99 %, Amberlyst resin, anisole (anhydrous) 99.7 %, methanol (HPLC grade), tetrahydrofuran (HPLC grade), n-hexane, ethanol, acetone (HPLC grade), toluene (anhydrous), Whatman 200 nm PTFE syringe filters were all purchased from Sigma-Aldrich and used without any further preparation. Sodium oleate (97%) was purchased from Tokyo Chemical Industry UK Ltd (TCI). CDCl_3 , D_2O and DMSO-d_6 solvents were purchased from GOSS Scientific. 0.25 inch, cubic neodymium–iron–boron rare earth magnets were purchased from Magcraft®.

Equipment

^1H NMR Spectroscopy: ^1H and ^{13}C NMR spectra were recorded in either DMSO-d_6 , CDCl_3 or D_2O using a 400 MHz Brüker Avance spectrometer. Chemical shifts (δ) are reported in parts per million (ppm) with respect to an internal reference of tetramethylsilane. **Triple Detection Size Exclusion Chromatography:** Triple detection SEC as performed using a Malvern Viscotek instrument equipped with a GPCmax VE2001 auto-sampler, two Viscotek T6000 columns (and a guard column), a refractive index (RI) detector VE3580 and a 270 Dual Detector (light scattering and viscometer) with a mobile phase of THF containing 2 v/v % of triethylamine and a flow-rate of 1 mL min^{-1} . **Dynamic light scattering:** DLS studies of nanoparticle dispersions were performed using a Malvern Zetasizer Nano ZS equipped with a 4 mW He–Ne, 633 nm at a temperature of 25°C and using plastic disposable cuvettes for aqueous dispersions. Malvern Zetasizer software version 6.20 was used for data analysis using the instruments automatic optimisation settings. It should be noted that measurements were taken directly from the nanoparticle dispersions ***without any additional filtration or centrifugation.*** **Zeta potential measurement:** Measurement of zeta potential also used the Malvern Zetasizer Nano ZS and were carried out at 1 mg mL^{-1} , at 25°C , at a pH of 6.5 using disposable capillary zeta cells; measurements were obtained using the instruments automatic optimisation settings. **Scanning Electron Microscopy:** SEM images were recorded using a Hitachi S-4800 FE-SEM at 3 kV. Aqueous nanoparticle solutions were pipetted onto aluminium stubs, clinical tissue was used to lightly dab the solution and the stubs were left to dry for approximately 3 hours, after which the dry samples were gold coated for 2 minutes at 15 mA using a sputter-coater (EMITECH K550X) prior to imaging. **Transmission Electron Microscopy (TEM).** TEM characterisation was carried out using a Hitachi S-4800 FE-SEM. TEM grids were prepared as follows; $10 \mu\text{L}$ of the particle dispersions were pipetted directly onto a holey carbon films on 400 mesh TEM grids (Agar Scientific) and immediately blotted away using a piece of filter paper. **Powder X-Ray Diffraction (PXRD)** was carried out using a Panalytical X'pert Pro multipurpose diffractometer with $\text{Co K}\alpha 1$ radiation ($\lambda = 1.789010 \text{ \AA}$). PXRD patterns were assigned using the JCPDS database. **Fourier-Transform Infrared (FT-IR) – Spectroscopy** was carried out using a Bruker Tensor 27 plate reading FT-IR. For each sample, 20 scans in the region from 650 to 4000 cm^{-1} were accumulated with a resolution of 4 cm^{-1} . **Thermogravimetric Analysis (TGA)** was carried out using a TA Instruments Q5000IR TGA under air atmosphere at 100 mL/min . 5–10 mg samples were heated to 120°C at 10°C/min and kept at 120°C for 20 min to remove all adsorbed solvent. The sample was then heated to 600°C at 10°C/min and kept at 600°C for 20 min. **Elemental Analysis.** The carbon and hydrogen

content of samples were analysed with a Thermo EA1112 Flash CHNS-O Analyzer. The measurement taken for the elemental content (%) was an average of four measurements. SQUID Analysis was carried out using a MPMS-XL-7 from Quantum Design. Dry samples were accurately weighed into a gel capsule (provided by the same company). Accurate SPION content was determined by ICP-OES (Spectro Ciros) by dissolution of the capsule following SQUID analysis in 5 mL of 5 M HCl followed by 10 mL water.

Synthesis and characterisation of linear and branched $p(\text{HPMA})$ by ambient temperature methanolic ATRP

For a typical ATRP synthesis of linear $p(\text{HPMA})$ (target $\text{DP}_n = 50$ monomer units), HPMA (7.39 g, 51.26 mmol), EBIB (0.2 g, 1.03 mmol; plus anisole as an internal standard if undertaking kinetic studies @ 20 w/v% based on HPMA feed) were added to a 100 mL round-bottomed flask fitted with a magnetic stirrer bar. Methanol (HPLC grade; 50 v/v% based on HPMA feed) was added and the solution degassed with a nitrogen purge for approximately 10 minutes whilst stirring. Cu(I)Cl (0.10 g, 1.03 mmol) and bpy (0.33 g, 2.10 mmol) were weighed together and quickly added to the stirring solution whilst maintaining a positive nitrogen flow. After initiation, the nitrogen flow was removed and the flask was made air-tight using parafilm. The solution was allowed to polymerise at ambient temperature. After approximately >99% conversion (judged by ^1H NMR analysis) the reaction was exposed to the atmosphere and manually terminated *via* THF addition (approximately 200 mL). Once fully terminated, Dowex Marathon exchange beads (~10 g) were added to the solution and stirred for approximately 20 minutes, in order to aid catalyst removal. The beads were removed by filtration and the remaining solution was passed over a basic alumina column to remove residual catalyst/ligand complex. The mixture was concentrated under vacuum which removed the majority of THF and the viscous solution was precipitated into cold hexane and filtered to yield white powders. For $p((\text{HPMA}_{50}\text{-co-EGDMA}_{0.8}))$, EGDMA (0.163 g, 0.83 mmol) was added to reaction mixture with HPMA and co-polymerisations were carried out using an identical protocol as above.

Synthesis and characterisation of linear and branched $p(\text{PEG}_x\text{-}b\text{-HPMA}_{50})$ block copolymers by ambient temperature methanolic ATRP

PEG_x-Br macroinitiator synthesis

A typical procedure for the preparation of a monomethoxy-capped poly(ethylene glycol) initiator (PEG_x-Br) is outlined as follows. PEG_x-OH (26.6 mmol, 1 eq.), toluene (anhydrous; 150 mL), 4-dimethylaminopyridine (DMAP; 0.32 g, 2.66 mmol, 0.1 eq.), and triethylamine (TEA; 4.08 mL, 2.96 g, 29.26 mmol, 1.1 eq.) were placed in a round-bottomed flask fitted with a magnetic stirrer bar. 2-Bromoisobutyl bromide (3.62 mL, 2.96 g, 29.26 mmol, 1.1 eq.) was added dropwise to the solution via a syringe over approximately 30 minutes. The solution was stirred overnight, after which Amberlyst resin A21 (20 g) was added to remove residual acid bromide and the mixture stirred for approximately one hour. The solution was then filtered to remove any insoluble material. Solvent was removed under vacuum from the resulting clear, pale yellow filtrate. The oily product was dried at 60 °C in a vacuum oven overnight and stored at ~4 °C. The method was slightly altered for the preparation of the higher molecular weight initiators as the initial toluene required warming to approximately 50 °C to dissolve the PEG_x-OH; products were purified by evaporation of the toluene to approximately one third volume before precipitation into cold petroleum ether (60-80); the

macroinitiators were collected on filter paper and dried under vacuum yielding white powdery products. NMR spectroscopic analysis of PEG_x-Br macroinitiators: ¹H NMR (CDCl₃): 1.94 ppm (ester CH₃), 3.38 ppm (methoxy CH₃), 3.50-3.80 (PEG backbone CH₂), 4.32 (CH₂-O-CO) - see Figure S1.

ATRP polymerisation of linear and branched p(PEG_x-b-HPMA) block copolymers

In a typical synthesis, PEG₁₁₇-Br initiator (0.94 g, 1.03 mmol) and HPMA (7.39 g, 51.26 mmol; target DP_n = 50 monomer units; plus anisole @ 20% w/v for kinetic studies) were placed into a 100 mL round-bottomed flask. HPLC grade methanol was added (50% w/v; initiator+monomer/solvent) and the solution was stirred/deoxygenated using a nitrogen purge for 10 minutes. Cu(I)Cl (0.10 g, 1.03 mmol) and bpy (0.19 g, 0.97 mmol) were added to the flask whilst maintaining a positive nitrogen pressure. After initiation, the nitrogen flow was removed and the flask was made air-tight using parafilm. The solution was allowed to polymerise at ambient temperature. After approximately >99% conversion (judged by ¹H NMR analysis) the reaction was exposed to the atmosphere and manually terminated *via* THF addition (approximately 200 mL). Once fully terminated, Dowex Marathon exchange beads (~10 g) were added to the solution and stirred for approximately 20 minutes, in order to aid catalyst removal. The beads were removed by filtration and the remaining solution was passed over a basic alumina column to remove residual catalyst/ligand complex. The mixture was concentrated under vacuum which removed the majority of THF and the viscous solution was precipitated into cold hexane and filtered to yield white powders. For branched block copolymers EGDMA (0.95 molar equivalents relative to initiator) was added to reaction mixtures with HPMA and co-polymerisations were carried out using an identical protocol as above. Example NMR spectroscopic analysis of *p*(PEG₁₇-*b*-HPMA₅₀): ¹H NMR (d₆-DMSO): 0.65-1.02 ppm, 1.02-1.26 ppm, 1.64-2.01 ppm, 3.22-3.26 ppm, 3.3-3.5 ppm, 3.49-3.54 ppm, 3.56-3.87 ppm, 4.53-4.71 ppm – see Figure S2.

Synthesis and characterisation of Iron Oxide Nanoparticles (SPIONs)

SPION synthesis was conducted (rather than purchasing of commercially available materials) as: 1) commercially available SPIONs were only available in water-immiscible solvents (eg toluene) which would not be suitable for the planned nanoprecipitations, 2) the scale of material required to conduct all experiments from a single batch of SPIONs was not cost effective with respect to commercial sources, 3) previous batches of commercial SPIONs have shown variable and often low magnetism, 4) exploratory experiments to exchange toluene-dispersed SPIONs to a THF medium led to irreversible aggregation.

Iron(III) Oleate Complex 10.8 g of iron(III) chloride hexahydrate (40 mmol) and 36.5 g sodium oleate (120 mmol) were dissolved in a mixture of deionised water (60 mL), ethanol (80 mL) and hexane (140 mL). The mixture was heated under reflux at 70 °C for 4 hours. Iron(III)-oleate was present in the resulting upper dark red organic layer, which was washed three times with deionised water (30 mL), dried over anhydrous magnesium sulphate and hexane removed via rotary evaporation. Elemental Analysis; Theory = C = 72.05%, H = 11.08% Calc = 68.64%, H = 10.36%. FT-IR: 722, 1300, 1434, 1521, 1586, 1709, 2853, 2922 and 3005 cm⁻¹. TGA weight loss = 88.97%. See Figures S8-9.

Oleic acid coated iron oxide nanoparticles. 7.08 g of the iron-oleate complex (8 mmol) and 1.19 g of oleic acid (4 mmol) were dissolved in 38.88 g (55 mL) of 1-octadecene at room temperature. The

mixture was heated to 320 °C at a heating rate of 3.3 °C min⁻¹, and maintained at 320 °C for 30 minutes. The resulting solution was then cooled to room temperature. 00 mL of ethanol was added to the black solution and the oleic acid coated iron oxide nanoparticles precipitated out. The nanoparticles were separated using a neodymium–iron–boron rare earth magnet and the solvent discarded. The resulting nanoparticles were subsequently re-dispersed in THF and stored as a solution of 7.24 mg/mL (in terms of inorganic content). The concentration was determined by TGA, described later) at 4°C. FT-IR bands; 1384, 1466, 2361, 2853 and 2923 cm⁻¹. DLS: (D_z) = 27 ± 2 nm, number average diameter (D_n) = 18 ± 2 nm, volume average diameter (D_v) = 21 ± 2 nm and Pdl = 0.23. Average Crystal size determined by PXRD = 8.05 ± 1.79 nm as derived from the Scherrer equation. Magnetisation saturation was determined by SQUID analysis as 43.61 emu/g. See Figures S10-14.

Determination of the concentration THF dispersion of oleic acid coated iron oxide nanoparticles. 50 mL of the oleic acid coated iron oxide nanoparticles dispersion in THF were pipetted onto a TGA plate. The sample was heated to 600 °C at 10 °C/min and kept at 600 °C for 20 min. The residual mass at 600 °C (therefore SPION) is 0.3622 mg, equating to 7.24 ± 0.07 mg/mL with respect to SPION. With respect to total combined mass, where the Oleic Acid : SPION ratio is 1.109 : 1 (described previously), the concentration is 15.27 mg/mL. See Figure S15.

Nanoprecipitation

Polymer Nanoprecipitation and Co-Nanoprecipitation of Polymer Incorporating 10 % w/w SPION. Polymers were dissolved in THF for a minimum of 24 hours at 5 mg/mL. Once dissolved 1 mL of polymer in THF was added quickly to a vial of water (5 ml) stirring at room temperature. This was immediately followed by either 69 mL of the 7.24 mg/mL SPION dispersion in THF (10 % w/w SPION) or 69 µL of THF (control). The solvent was allowed to evaporate overnight in a fume cupboard to give a final concentration of 1.1 mg/mL polymer/SPION nanocomposite particles or 1 mg/mL polymer nanoparticles in water. The presence of nanoparticle and size characteristics was determined by DLS without further dilution. See Figure S16.

Aggregation Studies

Magnetic nanoprecipitate response to applied magnetic fields. Magnetic nanocomposite dispersions were prepared as described above at 1.1 mg/mL. 1 mL was added to plastic disposable cuvettes with 1 cm path length. An initial DLS was taken using the instruments automatic optimisation settings in order to determine optimum attenuator and laser position settings. A neodymium–iron–boron rare earth magnet was coated with parafilm and suspended inside the cuvette, just touching the top of the liquid. The cuvette was placed inside the DLS spectrometer. The instrument's attenuator and laser position were set and fixed at the values previously determined from the initial scan. The sample's size measurements were recorded over a six hour period with a 10 minute delay between each scan. See Table S1 and Figures S17-20.

Reversible aggregation. Magnetic nanocomposite dispersions were prepared as described above at 1.1 mg/mL. 1 mL was added to plastic disposable cuvettes with 1 cm path length. In initial DLS measurement was taken using the instruments automatic optimisation settings in order to

determine optimum attenuator and laser position settings. A neodymium–iron–boron rare earth magnet was placed to the side of the cuvette for 24 hours. The cuvette was then carefully placed inside the DLS spectrometer so as not to disturb the aggregated magnetic material. The instrument's attenuator and laser position were set and fixed at the values previously determined from the initial scan and a DLS measurement was taken. The sample was then removed and gently shaken to re-disperse the aggregated magnetic nanocomposite particles. The cuvette was placed back into the DLS spectrometer and a second DLS measurement was taken at fixed attenuator and laser position. The process was repeated at 0, 24, 48 and 120 hours. See main manuscript and Figures S21-22.

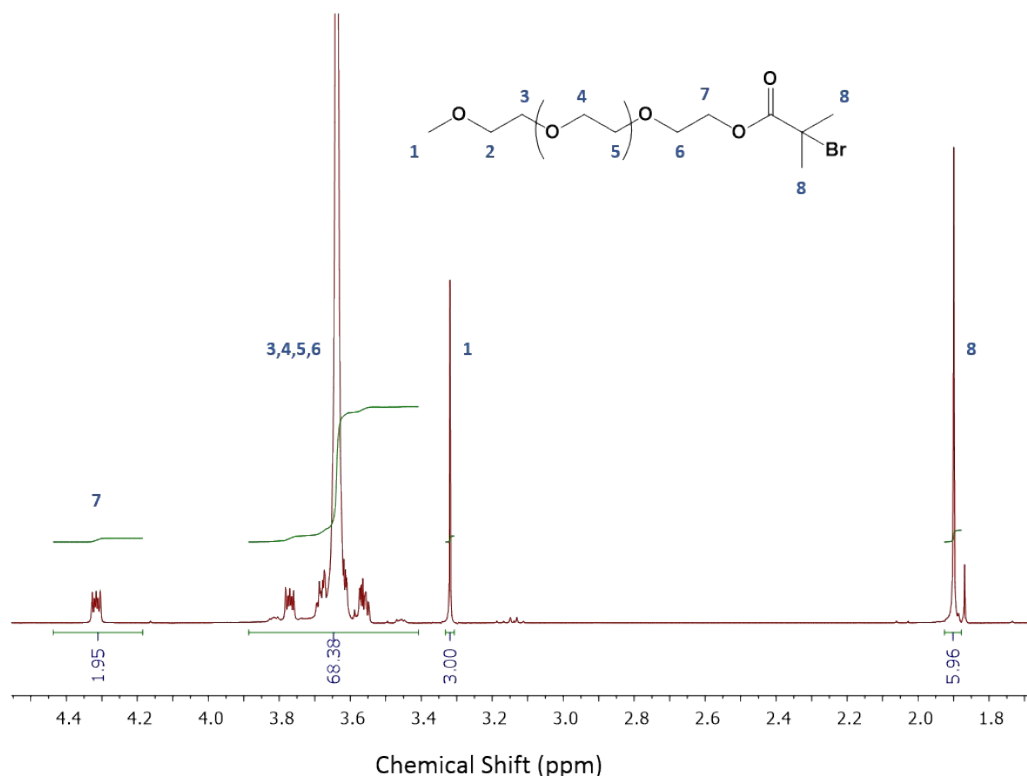


Figure S1. ^1H -NMR (D_2O) spectrum of PEG₁₇Br macroinitiator.

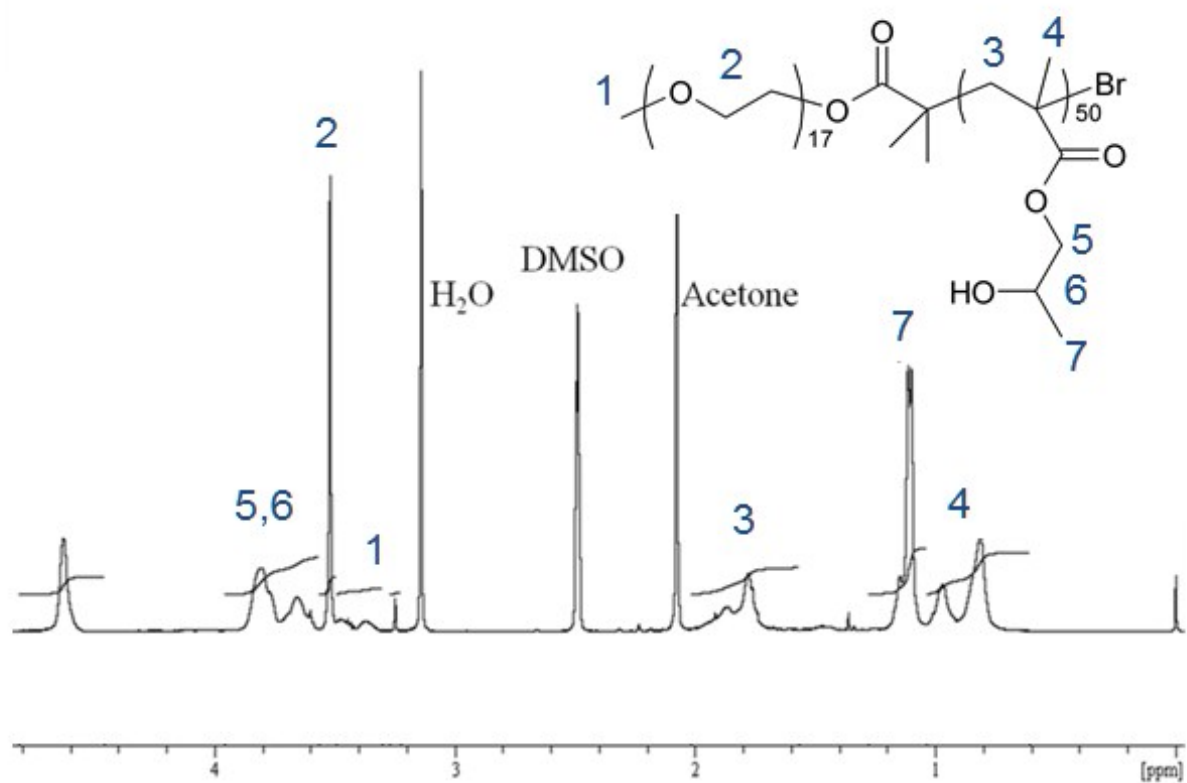


Figure S2. ^1H -NMR (DMSO-d_6) spectrum of $p(\text{PEG}_{17}\text{-}b\text{-HPMA}_{50})$ linear A-B block copolymer.

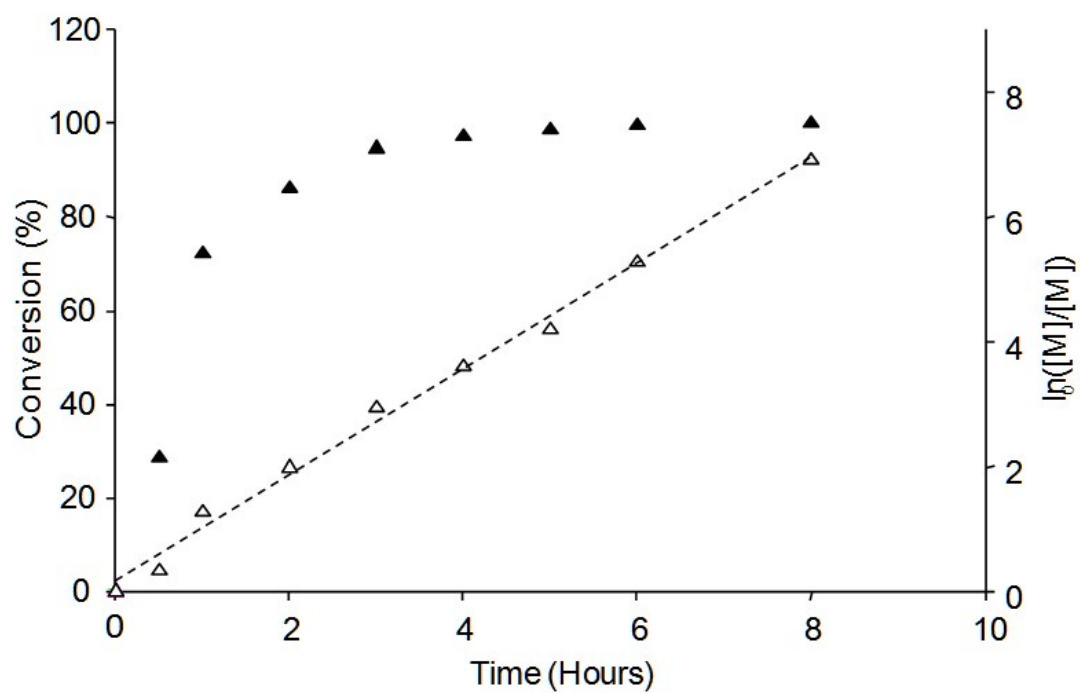


Figure S3. Kinetic studies of $p(\text{PEG}_{17}\text{-}b\text{-HPMA}_{50})$ synthesis *via* Cu-Catalysed ambient ATRP in methanol showing conversion and semilogarithmic plots vs. time.

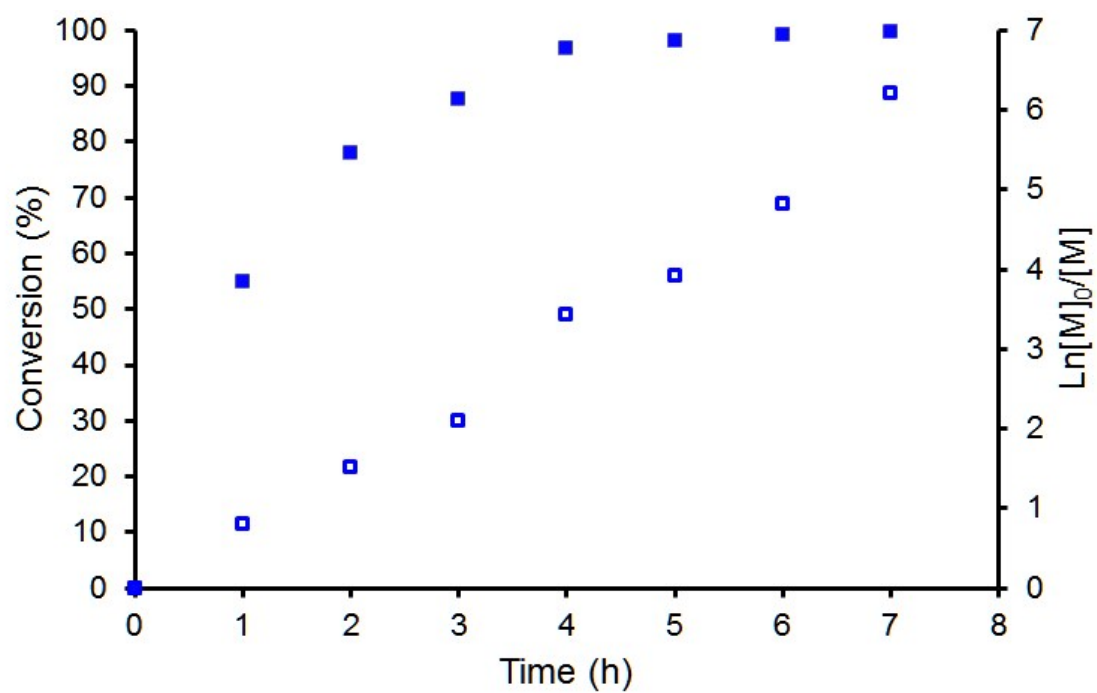


Figure S4. Kinetic studies of $p(\text{PEG}_{17}\text{-}b\text{-(HPMA}_{50}\text{-co-EGDMA}_{0.95}))$ synthesis *via* Cu-Catalysed ambient ATRP in methanol showing conversion and semilogarithmic plots vs. time.

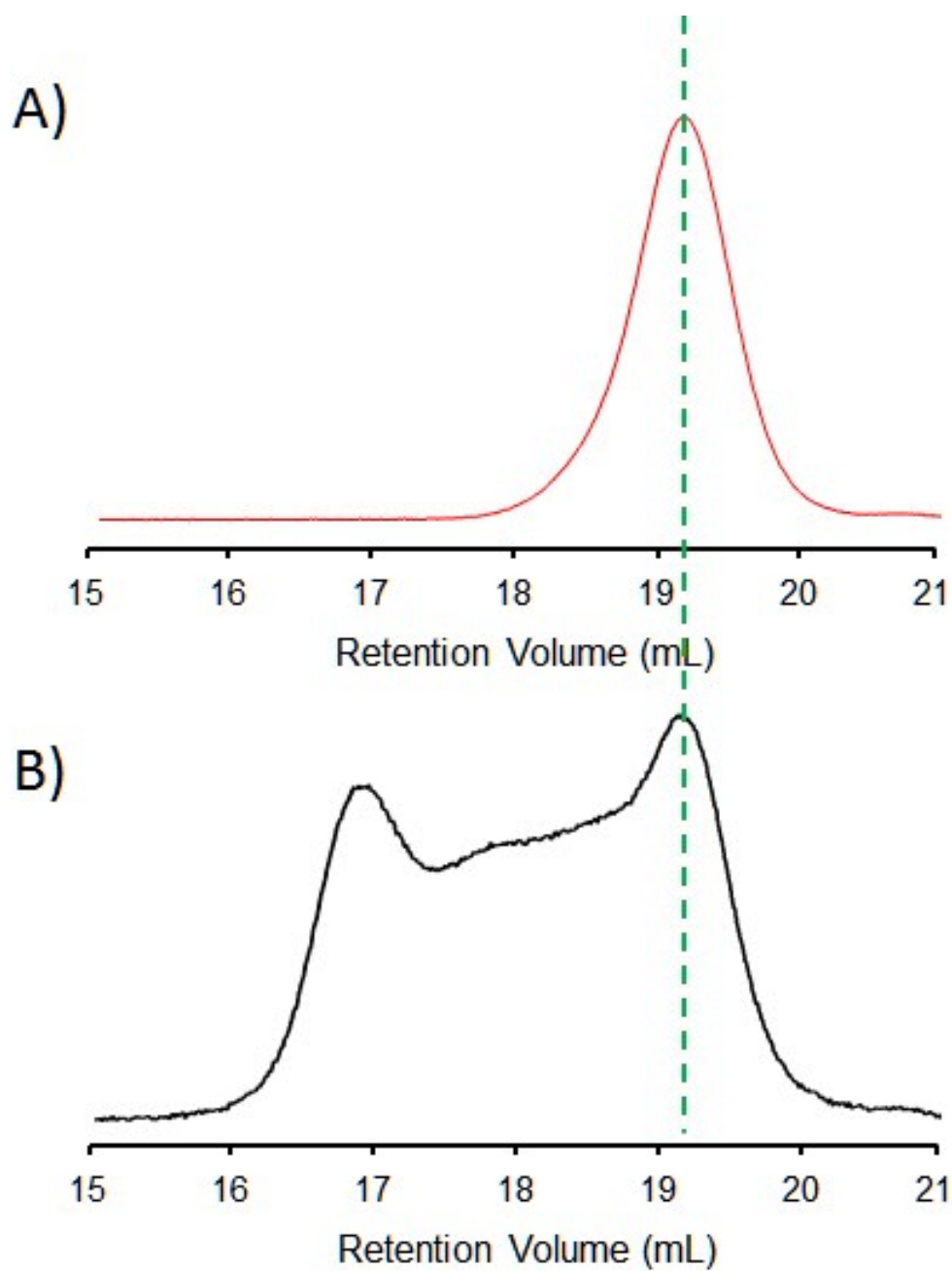


Figure S5. Overlaid SEC chromatograms (RI) of A) linear $p(\text{PEG}_{17}\text{-}b\text{-HPMA}_{50})$ and B) branched $p(\text{PEG}_{17}\text{-}b\text{-}(\text{HPMA}_{50}\text{-}co\text{-EGDMA}_{0.95}))$ A-B block copolymers. Analysis performed by triple detection SEC with a mobile phase of THF (+ TEA 2% v/v) at 1 mL/min.

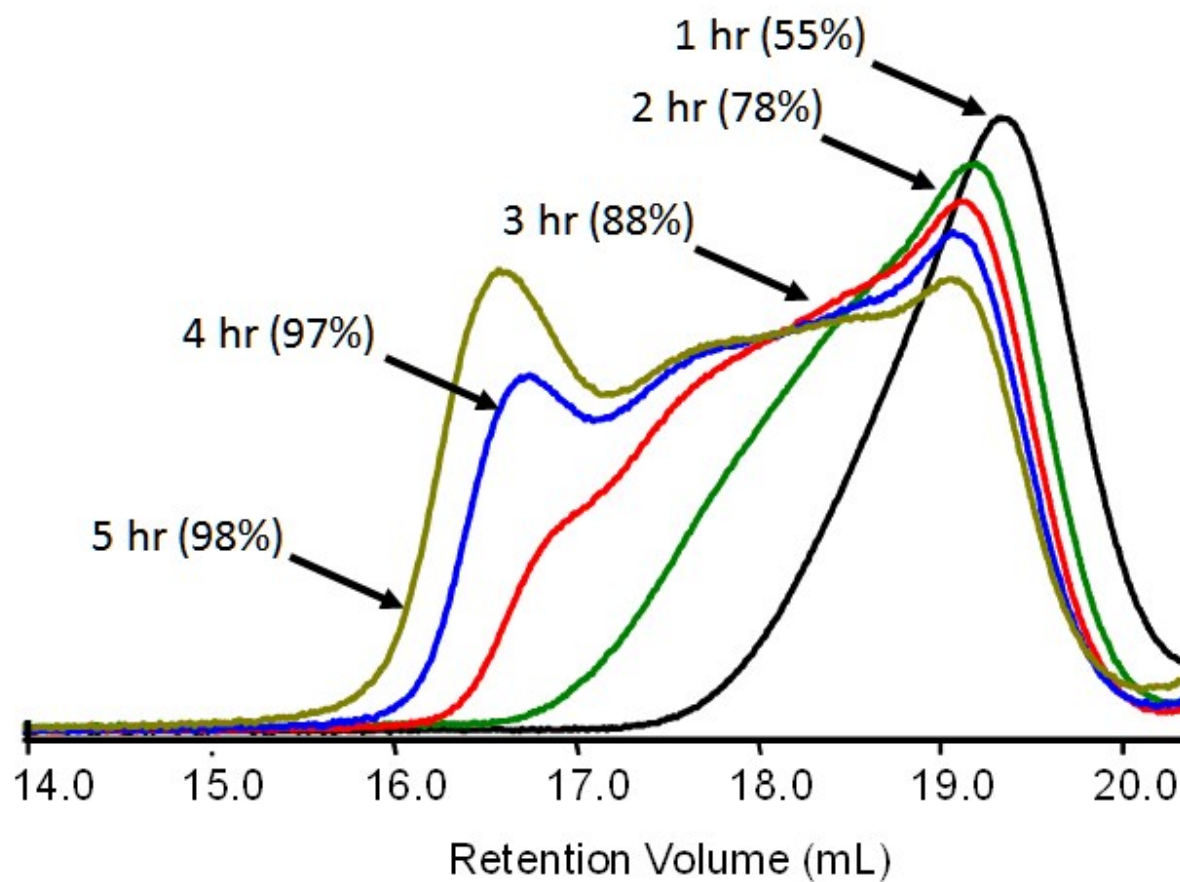


Figure S6. Overlaid SEC chromatograms (RI) of samples of $p(\text{PEG}_{17}\text{-}b\text{-(HPMA}_{50}\text{-}co\text{-EGDMA}_{0.95}))$ branched A-B block copolymer taken during synthesis *via* methanolic Cu-catalysed ambient ATRP. Analysis performed by triple detection SEC with a mobile phase of THF (+ TEA 2% v/v) at 1 mL/min.

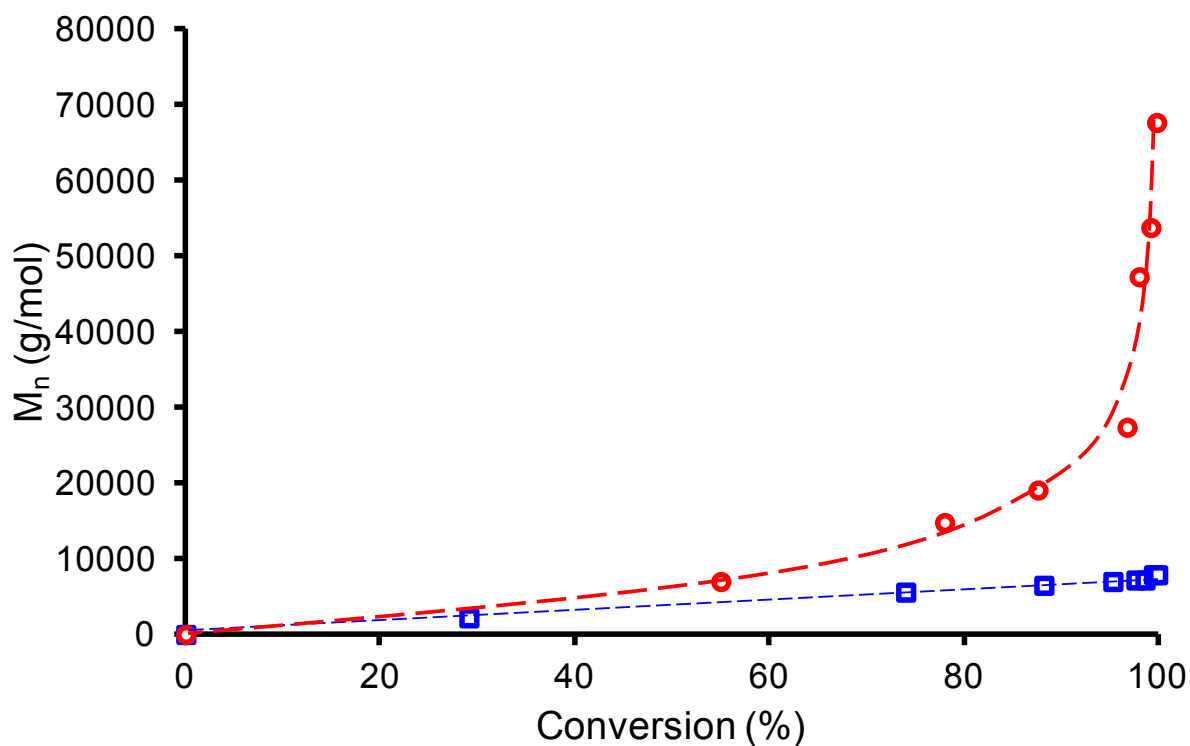


Figure S7. M_n vs. conversion plots for the synthesis of linear $p(\text{PEG}_{17}\text{-}b\text{-HPMA}_{50})$ (open blue squares) and branched $p(\text{PEG}_{17}\text{-}b\text{-(HPMA}_{50}\text{-co-EGDMA}_{0.95}))$ (open red circles) A-B block copolymers synthesised *via* Cu-Catalysed ambient ATRP in methanol.

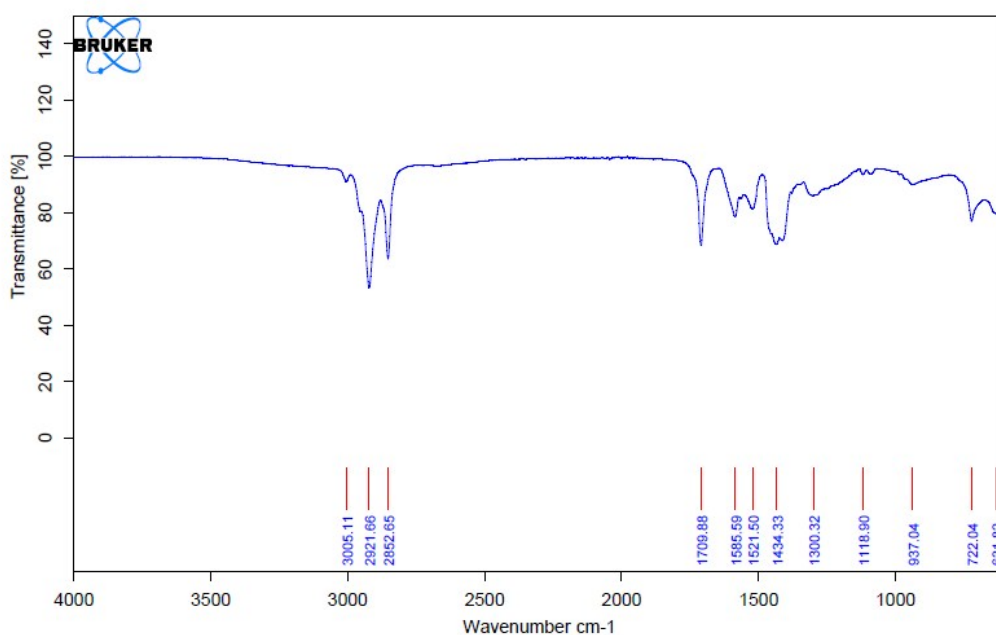


Figure S8. FT-IR spectrum of iron(III) oleate corresponding to previous reports (see ref 18 in main manuscript).

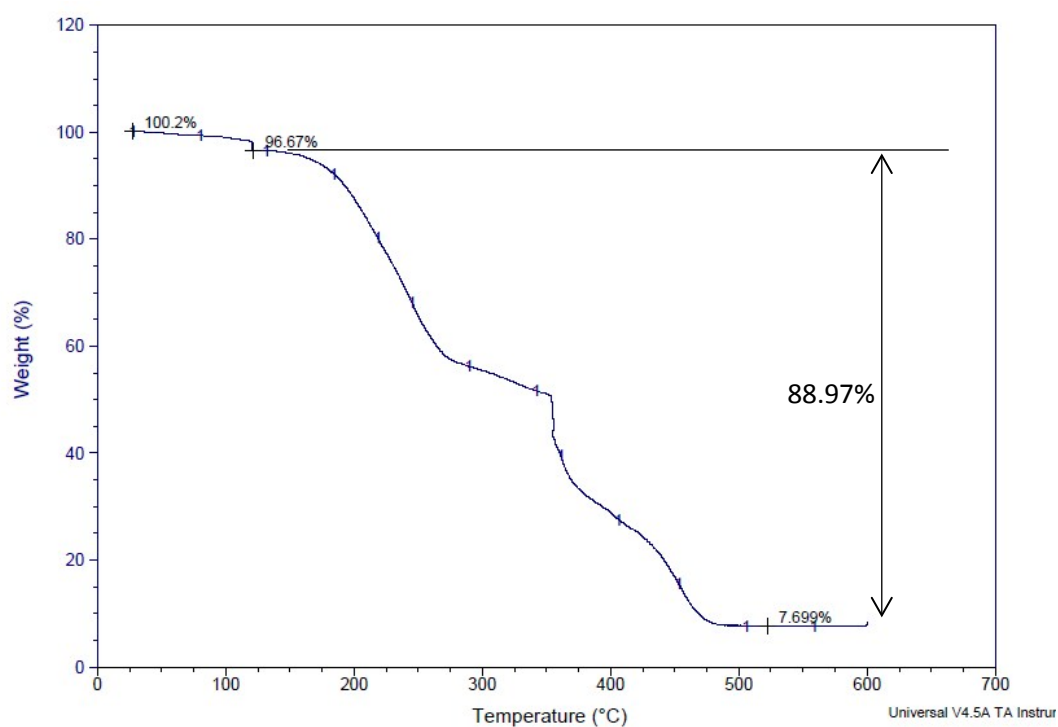


Figure S9. TGA analysis of iron(III) oleate (see ref 18 in main manuscript).

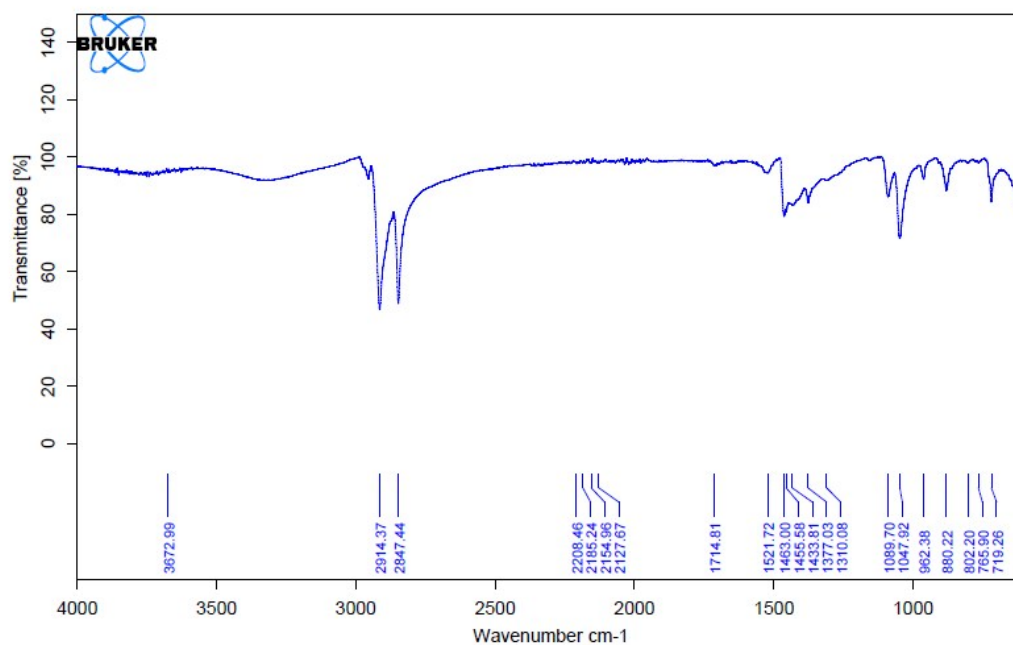


Figure S10. FT-IR spectrum of oleic acid coated iron oxide nanoparticles (see ref 18 in main manuscript).

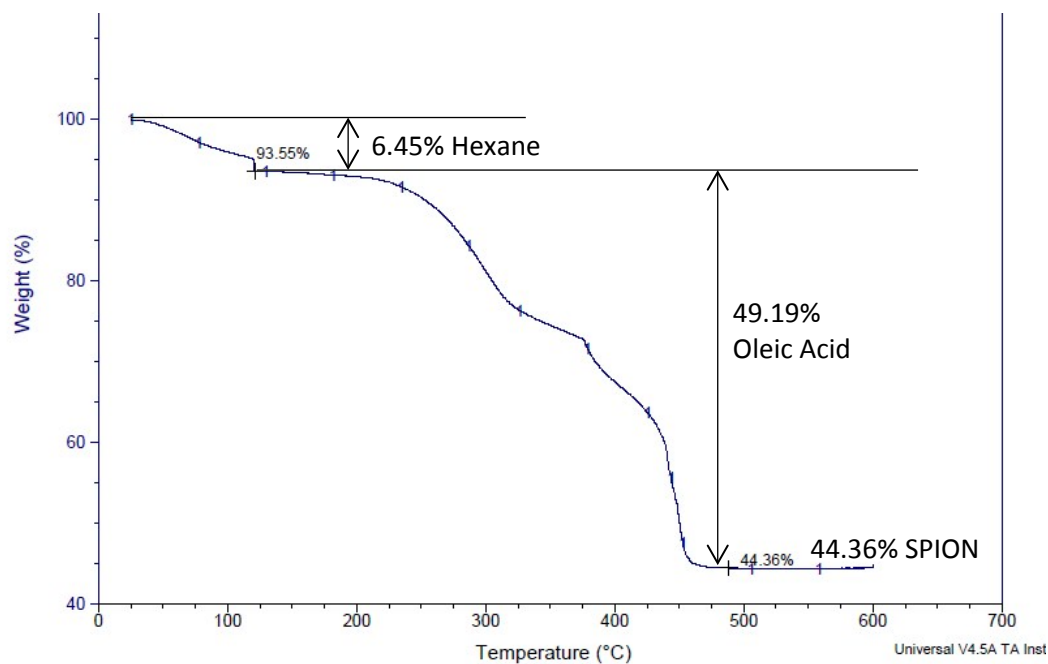


Figure S11. TGA analysis of oleic acid coated iron oxide nanoparticles; ratio 1.109 : 1 Oleic Acid : SPION (see ref 18 in main manuscript).

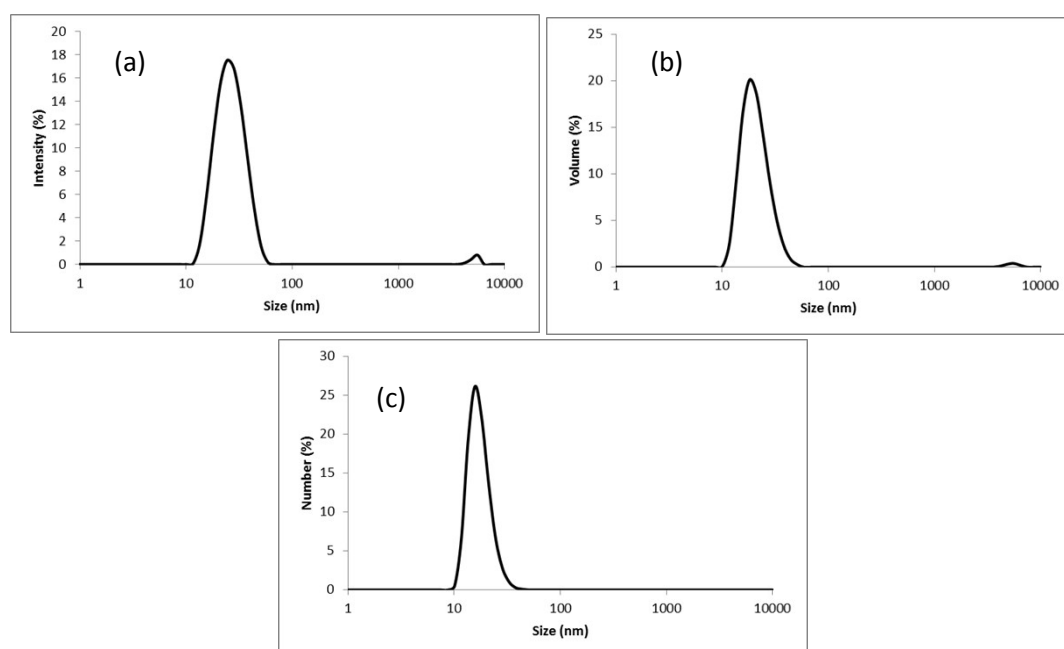


Figure S12. DLS analysis showing (a) D_z , (b) D_v and (c) D_n for oleic acid coated iron oxide nanoparticles. Samples dispersed at 0.1 mg/mL in THF at 25 °C.

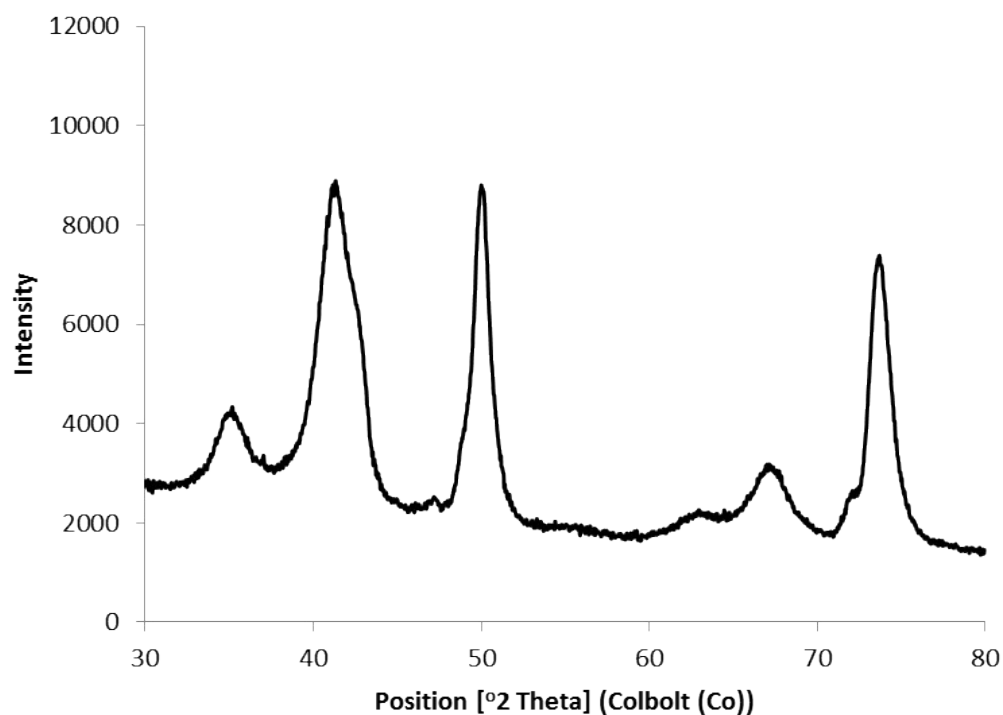


Figure S13. pXRD plot of SPIONs. The pXRD pattern shows crystalline material in good agreement with the reference pattern for magnetite (ICDD no. 00-019-0629) - (see ref 18 in main manuscript).

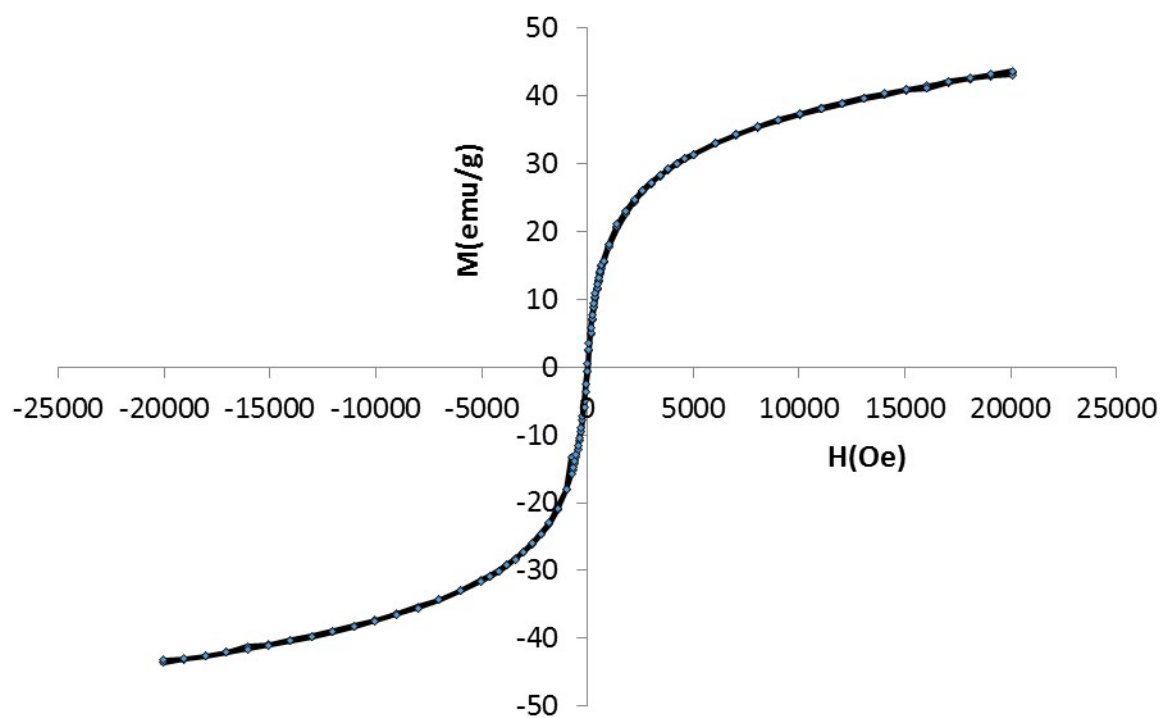


Figure S14. SQUID analysis of oleic acid coated iron oxide nanoparticles.

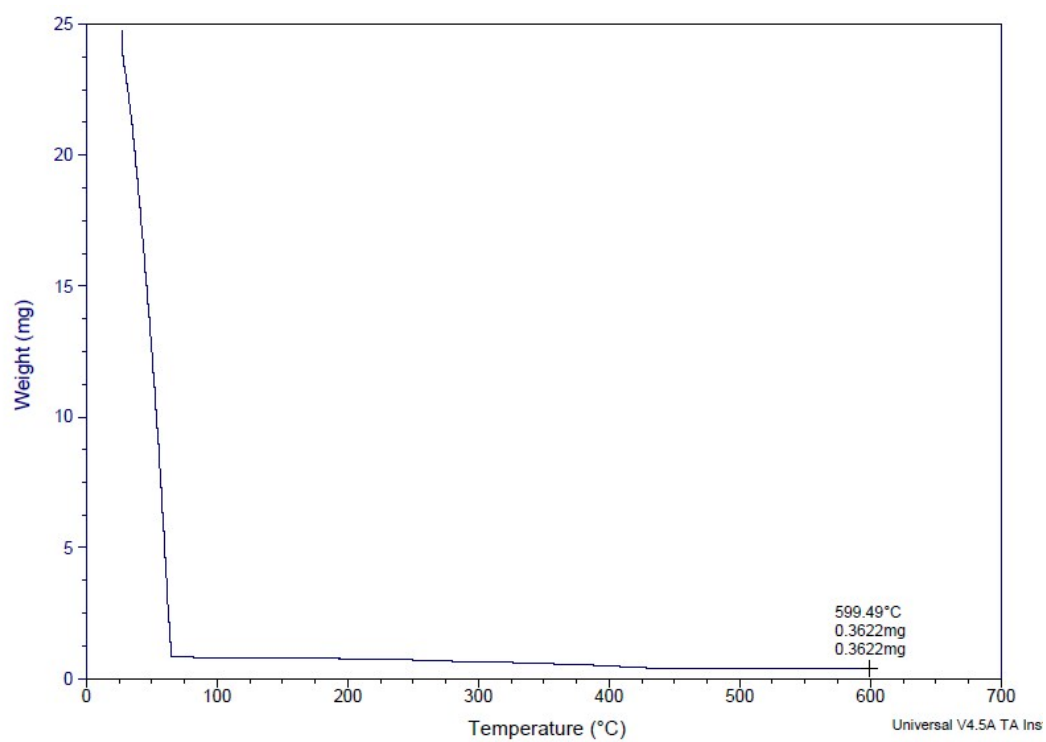


Figure S15. TGA analysis of Oleic acid coated iron oxide nanoparticles dispersed in THF.

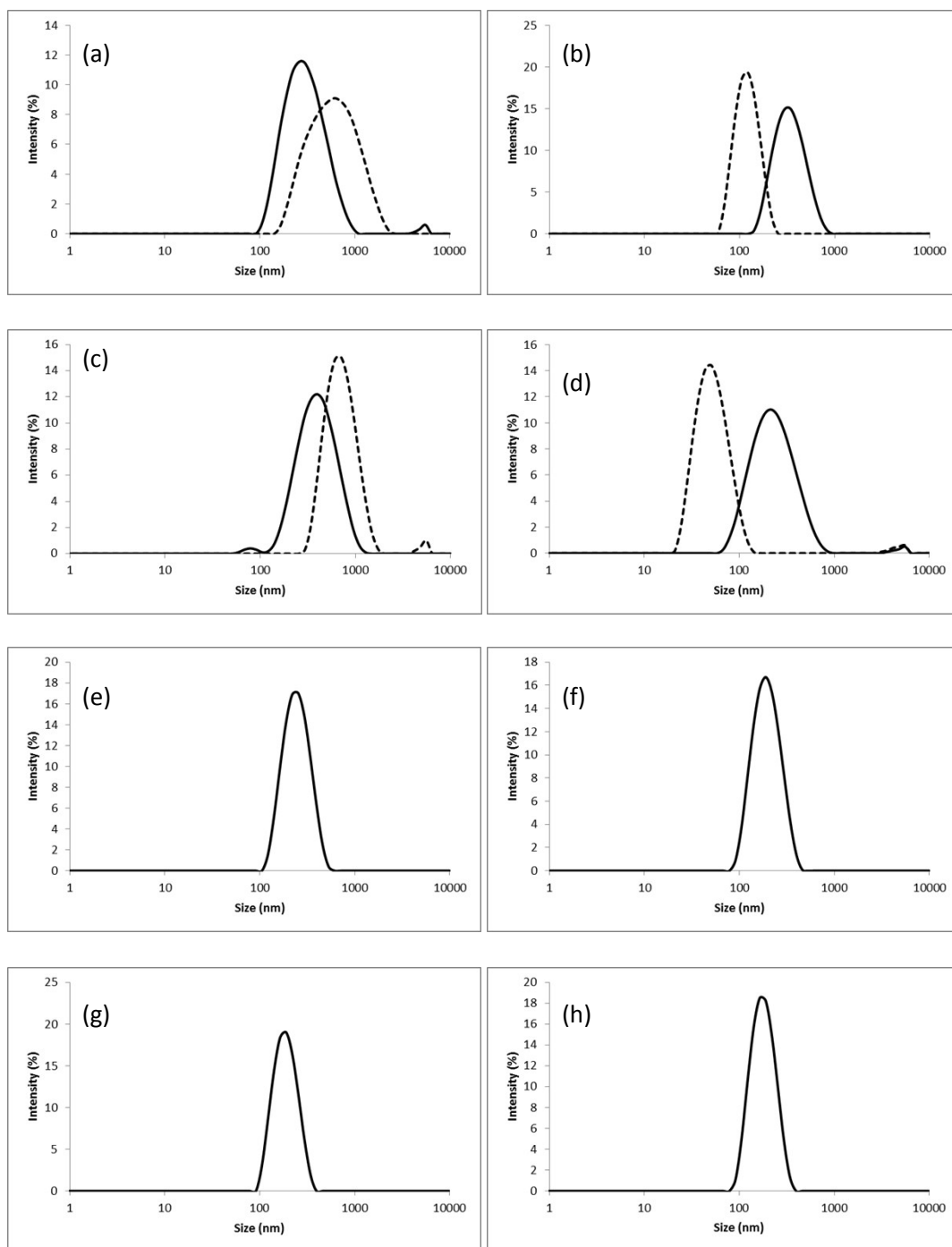


Figure S16. DLS analysis showing Dz for polymer nanoprecipitation (dashed line) and co-nanoprecipitation of polymer incorporating 10 % w/w SPION (solid lines) for (a) $p(\text{HPMA}_{50})$, (b) $p(\text{HPMA}_{50}\text{-co-EGDMA}_{0.8})$, (c) $p(\text{PEG}_{17}\text{-}b\text{-HPMA}_{50})$, (d) $p(\text{PEG}_{17}\text{-}b\text{-(HPMA}_{50}\text{-co-EGDMA}_{0.95}))$, (e) $p(\text{PEG}_{45}\text{-}b\text{-HPMA}_{50})$, (f) $p(\text{PEG}_{45}\text{-}b\text{-(HPMA}_{50}\text{-co-EGDMA}_{0.95}))$, (g) $p(\text{PEG}_{113}\text{-}b\text{-HPMA}_{50})$, (h) $p(\text{PEG}_{113}\text{-}b\text{-(HPMA}_{50}\text{-co-EGDMA}_{0.95}))$. DLS carried out at 1 mg mL^{-1} and 25°C .

Table S1 Time required for SPION-containing polymer-derived co-nanoprecipitates to reach 20% of their initial count rates when subjected to a suspended magnetic field.

Polymer composition	Time (mins) ^a
$p(\text{HPMA}_{50})$	26.0
$p(\text{PEG}_{17}\text{-}b\text{-(HPMA}_{50})$	28.4
$p(\text{PEG}_{45}\text{-}b\text{-HPMA}_{50})$	29.5
$p(\text{PEG}_{113}\text{-}b\text{-HPMA}_{50})$	50.3
$p(\text{HPMA}_{50}\text{-}co\text{-EGDMA}_{0.8})$	23.9
$p(\text{PEG}_{17}\text{-}b\text{-(HPMA}_{50}\text{-}co\text{-EGDMA}_{0.95})$	48.0
$p(\text{PEG}_{45}\text{-}b\text{-(HPMA}_{50}\text{-}co\text{-EGDMA}_{0.95})$	22.4
$p(\text{PEG}_{113}\text{-}b\text{-(HPMA}_{50}\text{-}co\text{-EGDMA}_{0.95})$	38.2

^aTime estimated from graphs shown in Figures S17-20

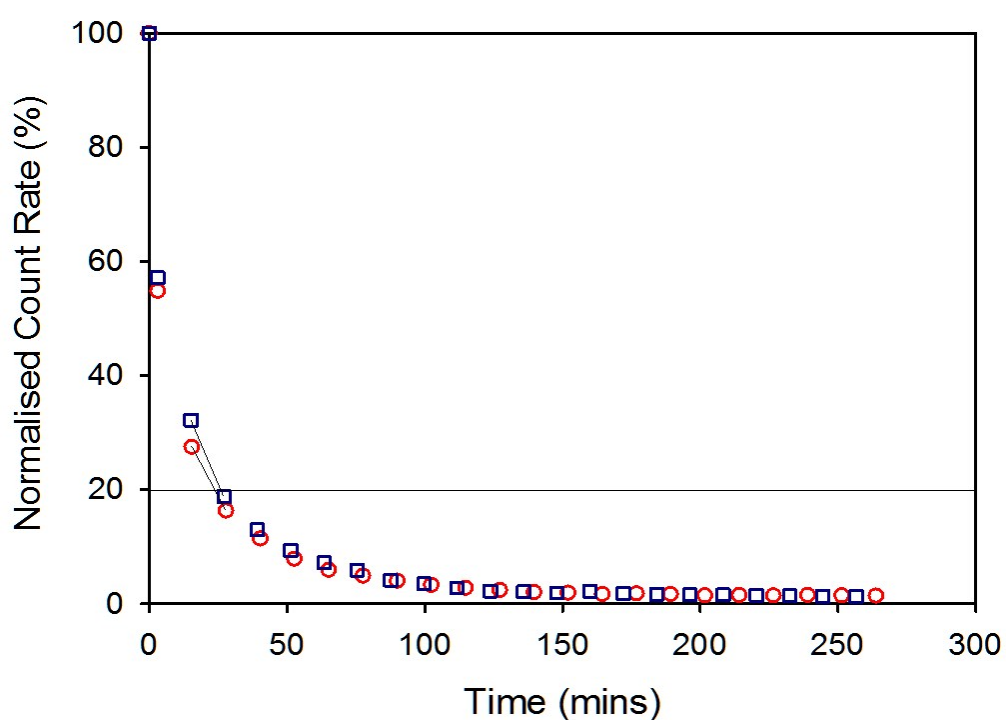


Figure S17. Normalised variation in count rate of SPION-containing nanoprecipitates comprising $p(\text{HPMA}_{50})$ (open blue squares) and $p(\text{HPMA}_{50}\text{-}co\text{-EGDMA}_{0.8})$ (open red circles) in the presence of a suspended magnetic field as measured by DLS. Analysis shows estimation of time taken to reach 20% of starting count rate, below which size determination is unreliable.

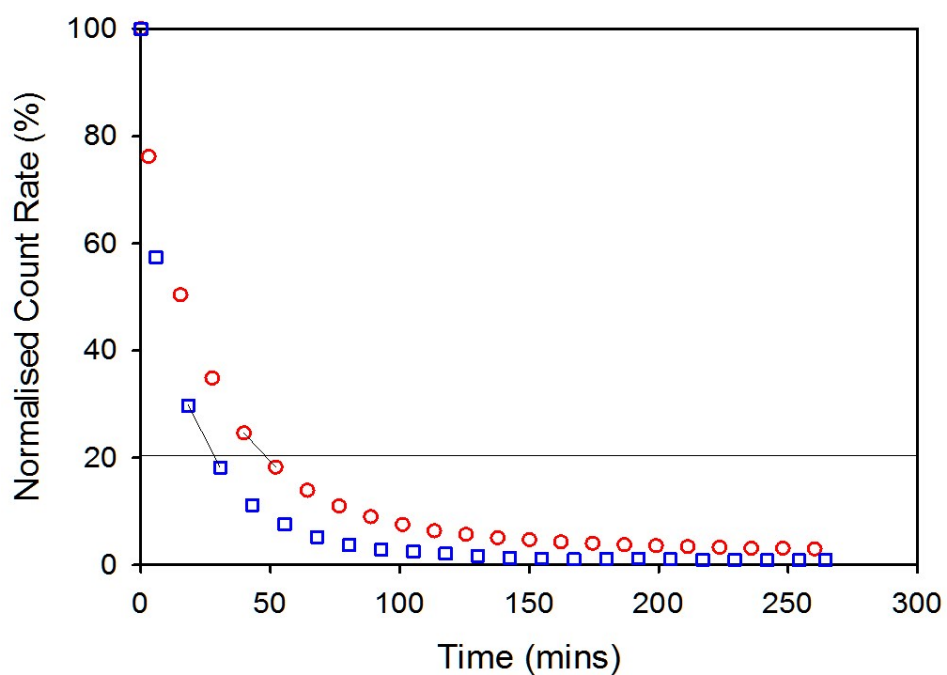


Figure S18. Normalised variation in count rate of SPION-containing nanoprecipitates comprising $p(\text{PEG}_{17}\text{-}b\text{-(HPMA)}_{50})$ (open blue squares) and $p(\text{PEG}_{17}\text{-}b\text{-(HPMA)}_{50}\text{-}co\text{-EGDMA}_{0.95})$ (open red circles) in the presence of a suspended magnetic field as measured by DLS. Analysis shows estimation of time taken to reach 20% of starting count rate, below which size determination is unreliable.

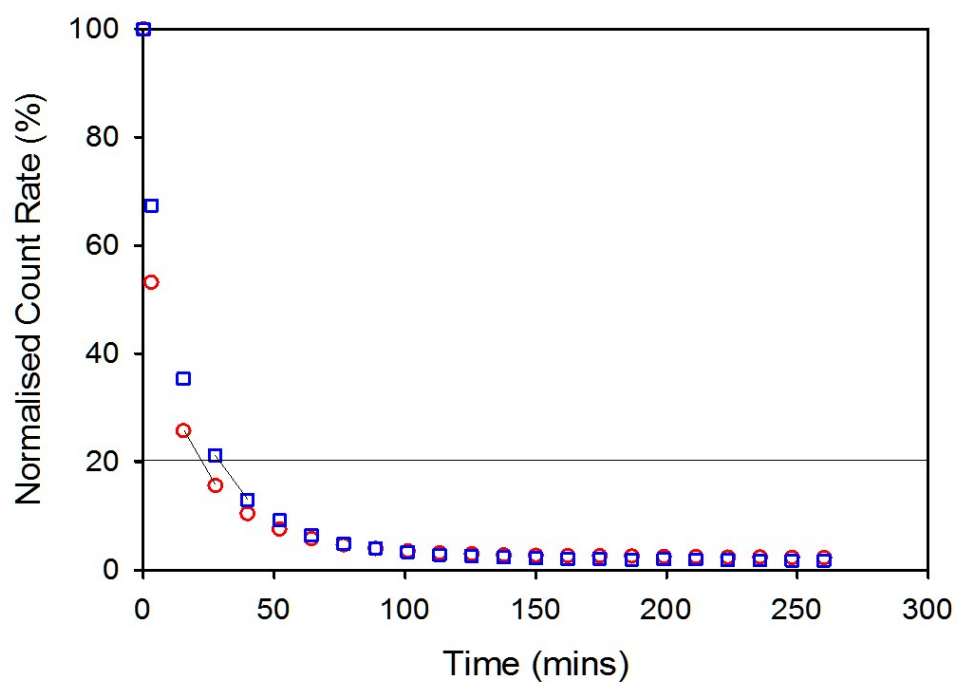


Figure S19. Normalised variation in count rate of SPION-containing nanoprecipitates comprising $p(\text{PEG}_{45}\text{-}b\text{-HPMA}_{50})$ (open blue squares) and $p(\text{PEG}_{45}\text{-}b\text{-(HPMA)}_{50}\text{-}co\text{-EGDMA}_{0.95})$ (open red circles) in the presence of a suspended magnetic field as measured by DLS. Analysis shows estimation of time taken to reach 20% of starting count rate, below which size determination is unreliable.

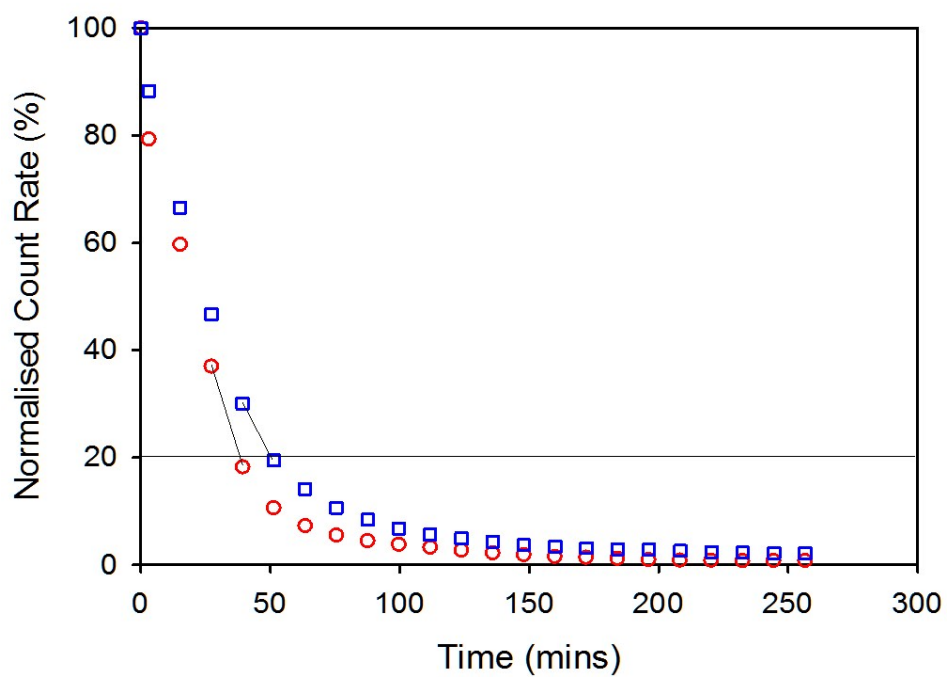


Figure S20. Normalised variation in count rate of SPION-containing nanoprecipitates comprising $p(\text{PEG}_{113}\text{-}b\text{-HPMA}_{50})$ (open blue squares) and $p(\text{PEG}_{113}\text{-}b\text{-(HPMA}_{50}\text{-}co\text{-EGDMA}_{0.95}))$ (open red circles) in the presence of a suspended magnetic field as measured by DLS. Analysis shows estimation of time taken to reach 20% of starting count rate, below which size determination is unreliable.

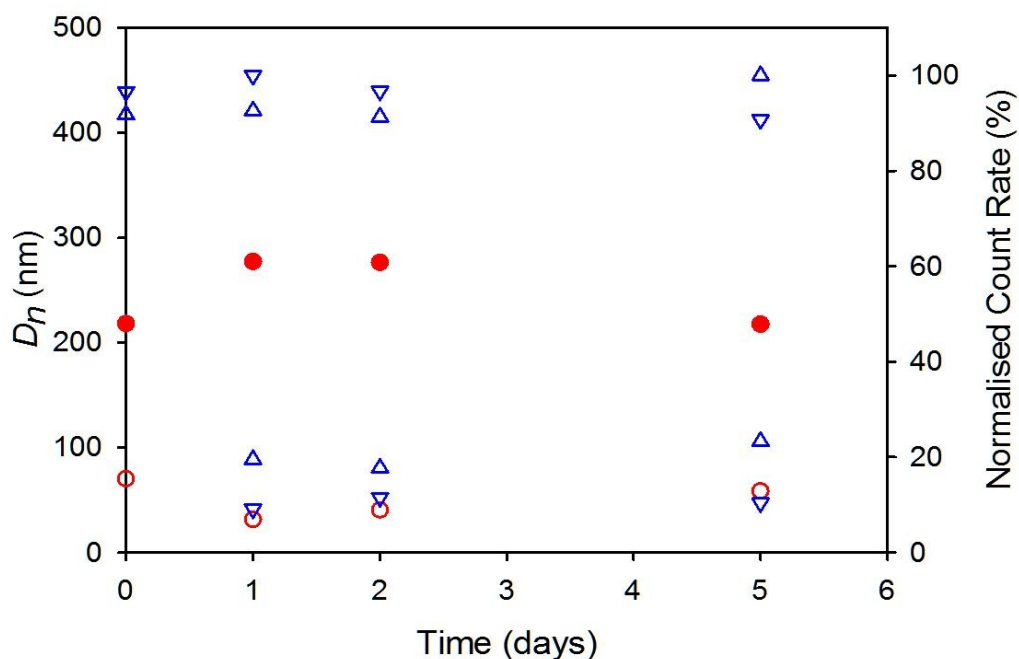


Figure S21. DLS studies of reversible aggregation and re-dispersion of SPION-containing nanoprecipitates comprising linear $p(\text{PEG}_{17}\text{-}b\text{-HPMA}_{50})$ (blue inverted triangles/filled red circles) and branched $p(\text{PEG}_{17}\text{-}b\text{-(HPMA}_{50}\text{-co-EGDMA}_{0.95}))$ (blue triangles/open red circles). Data shows three cycles of aggregation and re-dispersion over five days and resulting normalised count rates for both aggregated or re-dispersed samples and D_n values of re-dispersed samples.

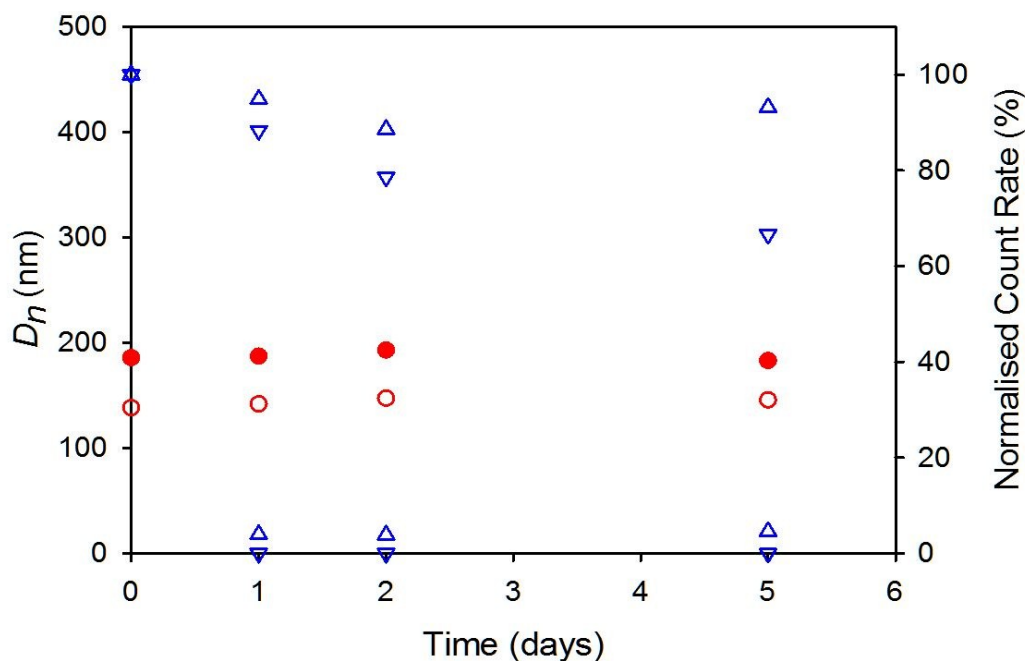


Figure S22. DLS studies of reversible aggregation and re-dispersion of SPION-containing nanoprecipitates comprising linear $p(\text{PEG}_{45}\text{-}b\text{-HPMA}_{50})$ (blue inverted triangles/filled red circles) and branched $p(\text{PEG}_{45}\text{-}b\text{-(HPMA}_{50}\text{-co-EGDMA}_{0.95}))$ (blue triangles/open red circles). Data shows three cycles of aggregation and re-dispersion over five days and resulting normalised count rates for both aggregated or re-dispersed samples and D_n values of re-dispersed samples.